

## GPPS-TC-2021-0124

### Boundary layer separation control of low-pressure turbine blades based on oscillating jet

**Luanliang Zhou**  
Shanghai Jiao Tong University  
sjtu\_zll@sjtu.edu.cn  
Shanghai, China

**Zifeng Jing**  
Shanghai Jiao Tong University  
jzfsjtu@sjtu.edu.cn  
Shanghai, China

**Xin Wen**  
Shanghai Jiao Tong University  
Wenxin84@sjtu.edu.cn  
Shanghai, China

**Yingzheng Liu**  
Shanghai Jiao Tong University  
yzliu@sjtu.edu.cn  
Shanghai, China

#### ABSTRACT

The Reynolds number ( $Re$ ) of the low-pressure turbine blades is low in the cruising state, and the laminar boundary layer of the suction surface is prone to separate from the action of the reverse pressure gradient. The separated laminar boundary layer may undergo transition and reattachment, and form laminar separation bubbles. Both situations will cause a lot of energy loss. Therefore, it is necessary to control the boundary layer of the low-pressure turbine with low  $Re$  Number. As a relatively new type of active flow control technology, the sweeping jet oscillator does not require moving parts and can generate high-frequency unsteady excitation at the outlet. With the capability of generating jets with a wide range of speeds and high frequencies and adapting to harsh environments with strong electromagnetic interference and radiation, it is an effective means of boundary layer control. From the results of experiments, we found that when  $Re$  is 10000, turbulence is 1.8% and the momentum coefficient controlled by the oscillating jet is 0.95%, the boundary layer can be reattached.

#### INTRODUCTION

When the low-pressure turbine works with a relatively low Reynolds number, the surface boundary layer is in a laminar flow state. At this time, the energy in the boundary layer is low, and the ability to resist the reverse pressure gradient is weak, which makes the boundary layer easy to flow separation. Flow separation will increase airfoil loss and reduce work efficiency (Bons, Benton et al. 2018). The boundary layer control of low-pressure turbine has two control methods, active control and passive control. Passive control methods mainly include: leading edge variants (Sangston, Little et al. 2014), passive vortex generators (Lake, King et al. 2000, Zhang, Vera et al. 2005), grooves (Lake, King et al. 2000), etc. The disadvantages of passive control methods are unable to adapt to other variable working conditions. The active control method can not only achieve the control effect with small energy, but also achieve precise control. Many active control methods are used for boundary layer control of low pressure turbines, such as continuous slit blowing (McAuliffe and Sjolander 2004), continuous vortex generators (Sondergaard, Rivir et al. 2002, Fernandez, Kumar et al. 2013), pulsed vortex generators (Bons, Sondergaard et al. 2000, Volino 2003, Bons, Plum et al. 2011, Mack, Brachmanski et al. 2013), zero net mass flow brakes (Volino 2003), Plasma brake (Huang, Corke et al. 2006).

The oscillating jet does not require any moving parts to generate high-frequency excitation. Because of its stable operation, simple structure, and adaptability to strong noise and pollution, it has attracted widespread attention from scholars (Kim, Kim et al. 2019, Wen, Liu et al. 2020, Wen, Liu et al. 2020, Tomac and Hossain 2021). In recent years, oscillating jets have been widely used in flow separation control (Jentsch, Taubert et al. 2019), combustion control (Bohan, Polanka et al. 2019), enhanced heat transfer (Mohammadshahi, Samsam-Khayani et al. 2020) and other fields. However, there is currently no research on the use of oscillating jets for flow control in low-pressure turbines.

This paper will use two test experimental methods to measure, including pressure scanning valve to measure the surface pressure distribution and particle image velocimetry to measure the surface flow field of the controlled low-pressure turbine, and to study the flow separation control of the low pressure turbine boundary layer based on the oscillating jet.

## METHODOLOGY

### 1. Experimental setup

The oscillator used in this paper is shown in Figure 1a. The operating principle of the oscillator is that when the main jet reaches the entrance throat, the main jet is attracted to one side wall due to the Coanda (Henri 1936) effect. A small part of the fluid near the jet outlet passes through the feedback channel and returns to the inlet of the oscillator, force the main jet to flip to the opposite side. Therefore, the jet exhibits periodic sweeping motion at the exit (Wen, Liu et al. 2019). Due to limitations on space in the LPT, it was necessary to ensure that the sweeping jet can still work normally in a small volume. Thus, a hot-wire anemometer was used to measure the frequency characteristics of the sweeping jets in the LPT. The experimental results are shown in Figure 1b. The outlet size of the sweeping jet actuator was 2 mm\*2 mm, and the oscillation frequency and outlet flow rate were found to vary linearly with respect to the volume flow rate in a small region, which follows traditional thinking(Tomac and Hossain 2021). 8 oscillators are arranged in an array with a spacing L of 20mm, the oscillators are located at 60% of the airfoil chord length, and the angle between the outlet and the airfoil is 30 °. The control parameters of the oscillator are expressed by the momentum coefficient  $C_{\mu}$ :

$$U_{jet} = \left( \dot{m} / \rho n_{jet} A_{jet} \right). \quad (1)$$

$$C_{\mu} = \dot{m} U_{jet} / q_{\infty} S_{ref}. \quad (2)$$

Where,  $U_{jet}$  represents the jet exit velocity,  $m$  represents the mass flow of the oscillating jet,  $\rho$  represents the density of compressed gas,  $n_{jet}$  represents the number of oscillating jets,  $A_{jet}$  represents the area of the oscillating jets,  $q_{\infty}$  represents the dynamic pressure of the free flow, and  $S_{ref}$  represents the airfoil reference area.

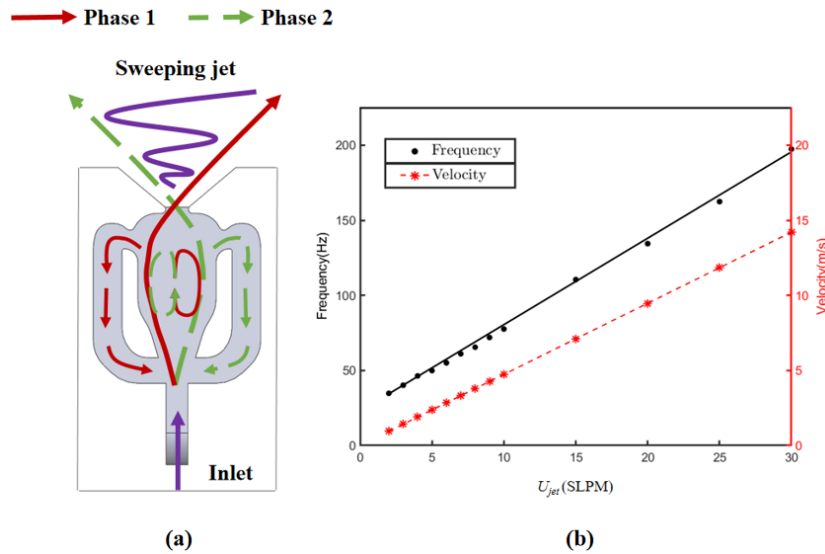
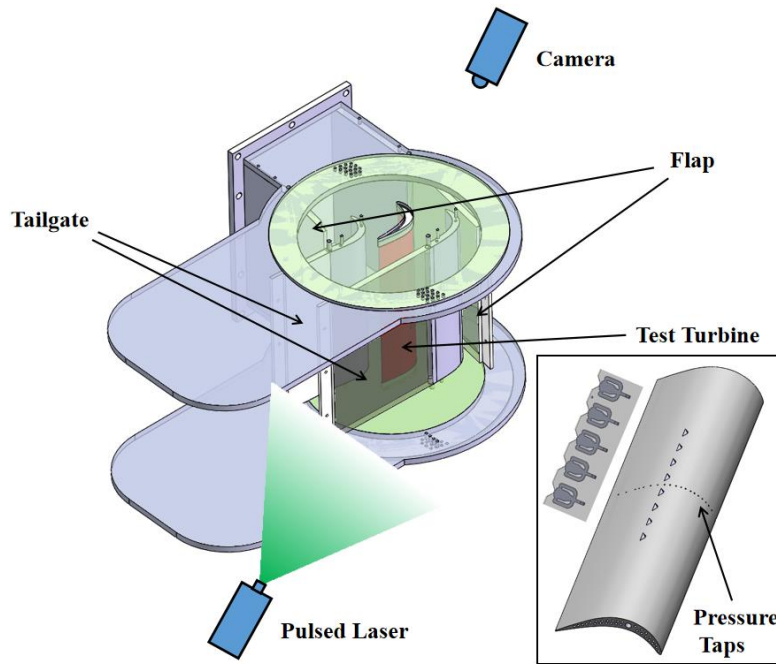


Figure 1 Experimental setup (a) Oscillating jet (b) The frequency of oscillating jet actuator

The experimental setup is shown in Figure 2. The low-pressure turbine is mounted on a variable-angle turntable, which can vary within  $\pm 10^\circ$  of the installation angle. Four flow control devices are used to adjust the flow into and out of the low-pressure turbine. Two flaps are used to draw the boundary layer and adjust the uniformity of the low-pressure turbine intake, while two tail plates are used to adjust the uniformity of the outlet flow. The four adjustment plates make the flow state of the middle low-pressure turbine closer to the real flow state. Please refer to the following chapters for detailed verification.

The airfoil used in this experiment is a ParkB airfoil profile, the chord length of the airfoil is 83.51mm, and the entrance angle is  $35^\circ$ . The low-pressure turbine test section consists of three airfoils. An oscillating jet array is set inside the middle airfoil. The compressed air can generate periodic oscillating jets at the outlet of the oscillator to control the

flow of the suction surface of the low-pressure turbine. The oscillating jet array is installed at 60% of the chord length of the low pressure turbine.



**Figure 2 Experimental setup**

## 2. Particle image velocimetry(PIV) setup

Except for the low-pressure turbine blades that are 3D printed and sprayed with black paint on the surface to prevent reflections, the other parts are made of transparent acrylic, which can make the laser light shine on the low-pressure turbine blades of interest through the adjusting plate. A particle generator is used to send the particles into the air inlet of the wind tunnel. The size of the particles is about 2-5 microns. For a Reynolds number of 10000, the time interval between laser pulses is 120 microns. Obtain a particle displacement of about 6-8 pixels, which is the most suitable algorithm for processing particle image velocimetry. Equipped with a 60mm focal length lens and a translation stage, the camera focuses on the laser plane. For each working condition, images are collected at a frequency of 5hz with a resolution of 2048\*2048, and a total of 1000 transient image pairs (2000 images) are used to analyze the average field.

## RESULTS AND DISCUSSION

### 1. Cp of no-controlled low-pressure turbine

As shown in Figure 3, the experimentally measured surface pressure coefficients under different Reynolds numbers are compared with (Corke, Thomas et al. 2007). The turbulence degree under the experimental conditions is 1.8%, and the turbulence degree in the reference is 1.6%. The experimental data corresponds well to the experimental results in [23], and the calculation formula of the surface pressure coefficient is as follows:

$$C_p = (P_{S,local} - P_{S,inlet}) / (P_{T,inlet} - P_{S,inlet}). \quad (3)$$

Where,  $P_{T,inlet}$  represents the free flow total pressure,  $P_{S,inlet}$  represents the free flow static pressure, and  $P_{S,local}$  represents the airfoil surface static pressure measured by the pressure measuring hole.

When Re is 10000 (Figure 3a), boundary layer flow separation occurs at the trailing edge of the airfoil suction surface. The separation point is defined as the position where the Cp value begins to appear a constant value, and the separation point is 70% chord length. When Re=25000 (Figure 3b), the separation point of the suction surface of the airfoil is about 70%, but it is found that at about 90% of the chord length, the slope of the suction surface increases significantly. According to the transition theory, transition occur in this area. Due to the increase in Reynolds number, the energy exchange between low-energy laminar boundary layer and high-energy fluid is enhanced, and the ability of the laminar boundary layer to overcome the inverse pressure gradient is enhanced. Transition occurs in the separated shear layer, but no boundary layer reattachment occurs at this time.

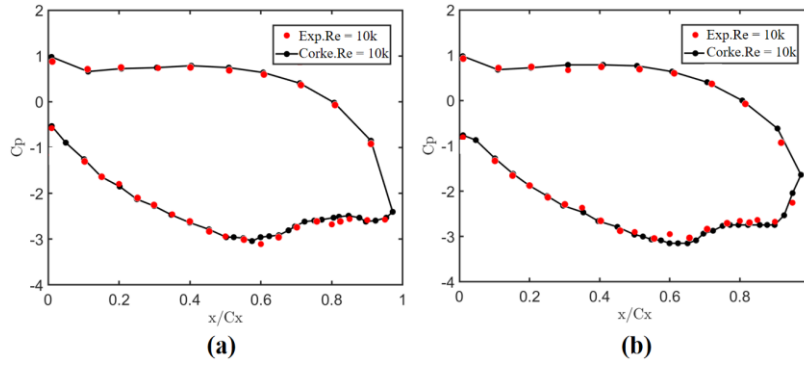


Figure 3 Surface pressure distribution of low-pressure turbine blades (a) Re=10k, (b) Re=25k

## 2. Cp of sweeping jet actuator control

Figure 4 shows the surface pressure coefficient  $C_p$  of a low-pressure turbine under the control of an oscillating jet. When  $C_{\mu}$  increases from 0.42% to 0.95%, the  $C_p$  changes very obviously, the plateau area starting at 70% chord length has disappeared, and the  $C_p$  from 65% chord length to 95% chord length is in a fully attached state. It shows that the oscillating jet can delay the separation and advance the transition, and reattach the separated boundary layer.

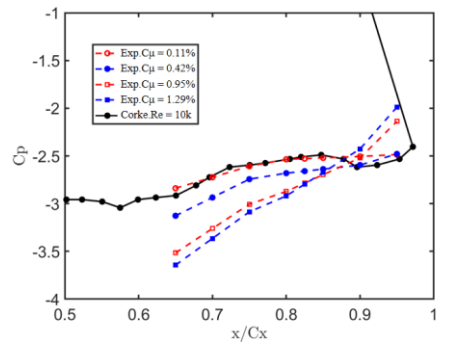
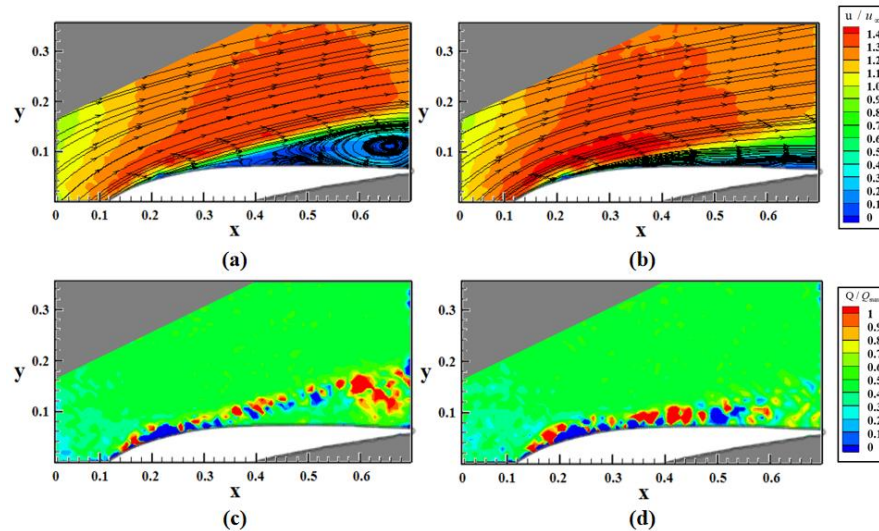


Figure 4 Surface pressure distribution of low-pressure turbine under the control of oscillating jet

## 3. PIV velocity average field and Q criterion vortex structure

Figure 5 shows the influence of the momentum coefficient  $C_{\mu}$  on the velocity average field and the Q-criterion vortex structure by Tecplot. With the increase of the momentum coefficient, the separation vortex in the trailing edge region of the airfoil is obviously reduced, and the separation boundary layer becomes thinner. When the momentum coefficient is 1.29% (Figure 5b), the boundary layer has been completely attached. Because the oscillator generates periodic oscillating jets at the outlet, which enhances the ability of the boundary layer to blend with high-energy fluids and enables the boundary layer to overcome the adverse pressure gradient. The Q criterion uses TECPLOT for post-processing calculations, and uses the maximum value for normalization. The oscillating jet forces the boundary layer to curl up into small vortices downstream of the exit position. These vortices fall off at the oscillating frequency and blend with the shedding vortex structure generated by the separation boundary layer, so that the higher momentum fluid enters the boundary layer, thereby maintaining time Evenly attach flow and reduce wake loss.



**Figure 5 The average velocity field and Q-criterion vortex structure under the control of oscillating jet by Tecplot (Re=10k, (a)  $C_{\mu}$ =0.11%, (b)  $C_{\mu}$ =1.29%, (c)  $C_{\mu}$ =0.11%, (d)  $C_{\mu}$ =1.29%)**

## CONCLUSIONS

In this study, surface pressure measurement and particle image velocimetry (PIV) experiments were performed on a typical low-pressure turbine airfoil ParkB, and the effect of Re number on flow separation under uncontrolled flow separation and the characteristics of airfoil surface flow field under oscillating jet control were analyzed. The main conclusions are as follows:

1. For uncontrolled airfoils, Re has a great influence on flow separation. At low Reynolds number (Re=10k), the separated boundary layer presents a larger separation bubble structure in the trailing edge region. With the increase of Reynolds number, the energy and momentum exchange between the laminar boundary layer and the external high-energy fluid becomes more intense. The separated boundary layer gradually adheres to the airfoil surface.

2. When Re=10k, the boundary layer can reattach and the separation bubble structure disappears when the oscillating jet  $C_{\mu}$ =0.95%. This is because the oscillating jet produces a continuous sweeping jet at the outlet, which can periodically swing at the jet outlet. The periodic sweeping behavior can break the large vortex structure produced by the flow separation, and gradually mix and dissipate with the surrounding fluid. The strong unsteadiness of the surface of the low-pressure turbine blade caused by the oscillating jet can promote the exchange of energy and momentum, and further control the reattachment of the separated boundary layer to the surface of the blade.

## ACKNOWLEDGMENTS

The authors also thank the financial support from the National Natural Science Foundation of China (Grant nos. 12072196) and Science and Technology Commission of Shanghai Municipality (Grant no. 19JC1412900) extended to this study

## References

- Bohan, B. T., M. D. Polanka and J. L. Rutledge (2019). "Sweeping Jets Issuing From the Face of a Backward-Facing Step." *Journal of Fluids Engineering-Transactions of the Asme* **141**(12).
- Bons, J., S. Benton, C. Bernardini and M. Bloxham (2018). "Active Flow Control for Low-Pressure Turbines." *AIAA Journal* **56**(7): 2687-2698.
- Bons, J. P., J. Pluim, K. Gompertz, M. Bloxham and J. P. Clark (2011). "The Application of Flow Control to an Aft-Loaded Low Pressure Turbine Cascade With Unsteady Wakes." *Journal of Turbomachinery* **134**(3).
- Bons, J. P., R. Sondergaard and R. B. Rivir (2000). "Turbine Separation Control Using Pulsed Vortex Generator Jets." *Journal of Turbomachinery* **123**(2): 198-206.
- Corke, T. C., F. O. Thomas and J. Huang (2007). "Documentation and Control of Flow Separation on a Low Pressure Turbine Linear Cascade of Pak-B Blades Using Plasma Actuators."
- Fernandez, E., R. Kumar and F. Alvi (2013). "Separation Control on a Low-Pressure Turbine Blade using Microjets." *Journal of Propulsion and Power* **29**(4): 867-881.
- Henri, C. (1936). Device for deflecting a stream of elastic fluid projected into an elastic fluid, US.
- Huang, J., T. C. Corke and F. O. Thomas (2006). "Plasma Actuators for Separation Control of Low-Pressure Turbine Blades." *AIAA Journal* **44**(1): 51-57.
- Jentsch, M., L. Taubert and I. Wygnanski (2019). "Using Sweeping Jets to Trim and Control a Tailless Aircraft Model." *Aiaa Journal* **57**(6): 2322-2334.
- Kim, S. H., H. D. Kim and K. C. Kim (2019). "Measurement of two-dimensional heat transfer and flow characteristics of an impinging sweeping jet." *International Journal of Heat and Mass Transfer* **136**: 415-426.

Lake, J., P. King and R. Rivir (2000). Low Reynolds number loss reduction on turbine blades with dimples and V-grooves. Aerospace Sciences Meeting & Exhibit.

Lake, J., P. King and R. Rivir (2000). Low Reynolds number loss reduction on turbine blades with dimples and V-grooves. 38th Aerospace Sciences Meeting and Exhibit.

Mack, M., R. Brachmanski and R. J. A. S. o. M. E. Niehuis (2013). "The Effect of Pulsed Blowing on the Boundary Layer of a Highly Loaded Low Pressure Turbine Blade." V06AT36A015.

McAuliffe, B. R. and S. A. Sjolander (2004). "Active Flow Control Using Steady Blowing for a Low-Pressure Turbine Cascade." Journal of Turbomachinery **126**(4): 560-569.

Mohammadshahi, S., H. Samsam-Khayani, O. Nematollahi and K. C. Kim (2020). "Flow characteristics of a wall-attaching oscillating jet over single-wall and double-wall geometries." Experimental Thermal and Fluid Science **112**.

Sangston, K., J. Little, M. E. Lyall and R. Sondergaard (2014). "End Wall Loss Reduction of High Lift Low Pressure Turbine Airfoils Using Profile Contouring—Part II: Validation." Journal of Turbomachinery **136**(8).

Sondergaard, R., R. B. Rivir and J. P. Bons (2002). "Control of Low-Pressure Turbine Separation Using Vortex-Generator Jets." **18**(4): 889-895.

Tomac, M. N. and M. A. Hossain (2021). "Flow and Frequency Characterization of the Synchronized Stacked Sweeping Jets." AIAA Journal **59**(1): 118-130.

Volino, R. J. (2003). "Separation Control on Low-Pressure Turbine Airfoils Using Synthetic Vortex Generator Jets." Journal of Turbomachinery **125**(4): 765-777.

Wen, X., J. Liu, D. Kim, Y. Liu and K. C. Kim (2020). "Study on three-dimensional flow structures of a sweeping jet using time-resolved stereo particle image velocimetry." Experimental Thermal and Fluid Science **110**.

Wen, X., J. Liu, Z. Li, D. Peng, W. Zhou, K. C. Kim and Y. Liu (2020). "Jet impingement using an adjustable spreading-angle sweeping jet." Aerospace Science and Technology **105**.

Wen, X., J. Liu, Z. Li, W. Zhou and Y. Liu (2019). "Flow dynamics of sweeping jet impingement upon a large convex cylinder." Experimental Thermal and Fluid Science **107**: 1-15.

Zhang, X. F., M. Vera, H. Hodson and N. Harvey (2005). "Separation and Transition Control on an Aft-Loaded Ultra-High-Lift LP Turbine Blade at Low Reynolds Numbers: Low-Speed Investigation." Journal of Turbomachinery **128**(3): 517-527.

#### **APPENDIX A - COPYRIGHT/OPEN ACCESS**

The GPPS policy is that all articles will be Open Source accessible. This article will be published using the Creative Commons Attribution [CC-BY 4.0](https://creativecommons.org/licenses/by/4.0/), thus allowing the author(s) to retain their copyright.

For answers to frequently asked questions about Creative Commons Licences, please see <https://creativecommons.org/faq/>.

#### **APPENDIX B - GPPS Presenter Policy and Paper Acceptance**

According to GPPS's presenter attendance policy, a paper cannot be published or be indexed and may not be cited as a published paper until at least one author pays the registration fee and attends the conference. The GPPS reserves the right to withdraw from its publications any paper that is not presented by an author of the paper at the appropriate conference. Any paper that is withdrawn may not be cited as a published paper.